Computers & Operations Research 42 (2014) 83–94

Contents lists available at ScienceDirect

Computers & Operations Research

journal homepage: www.elsevier.com/locate/caor

Characterizing multi-event disaster resilience

Christopher W. Zobel *, Lara Khansa

Department of Business Information Technology, Virginia Polytechnic Institute and State University, Blacksburg, VA 24061-0235, United States

ARTICLE INFO

Available online 10 October 2011

Keywords:
Predicted resilience
Disaster operations management
Quantitative modeling
Sudden-onset disasters

ABSTRACT

This paper presents an approach for providing a quantitative measure of resilience in the presence of multiple related disaster events. It extends the concepts of the resilience triangle and predicted disaster resilience by considering the tradeoffs between multiple criteria for each individual sub event, as well as for an entire multi event situation. The focus of the research is on sudden onset disasters, and on the initial impact of each sub event as well as the amount of time available to work towards recovery of the system before the next sub event occurs. A mathematical model is developed for the new resilience measure, along with an approach for graphically representing the relationships between the different criteria. An example is then provided of using the new approach to compare the relative resilience of different scenarios under a representative multi event disaster situation. The results demonstrate that characterizing multi event resilience analytically can ultimately provide a great depth of information and thus support better disaster planning and mitigation.

1. Introduction

The potential for significant loss of life resulting from improper preparedness and/or response to sudden onset disasters calls for effective quantification of system resilience. Such resilience can be considered both at a local level and on a larger scale, and in particular, the resilience of systems such as key supply chain networks is critical to the sustainability of society. These net works provide vital human services including water and medical supplies, energy resources (i.e. electric power, oil, gas, fuel, etc…), transportation capabilities, information and communication tech nologies, and currency exchange functionality [1,2]. The ability to quantify their resilience is instrumental in improving both emer gency planning and response by being able to compare various configurations and to assess their relative returns and risks for effective emergency management [3].

The focus of this paper is on quantifying system resilience to sudden onset disasters that are followed by multiple related sub disasters. Such situations include (1) natural disasters such as earthquakes and their aftershocks, along with related events such as delayed building collapses; and hurricanes with levee failures and the associated disruptions in transportation networks and power grids [4,5], (2) human made disasters such as terrorist attacks [6,7] and information security attacks [8] on stock exchanges, which could lead to serious price fluctuations and result in panic and financial meltdown, and (3) cascading network effects such as supply chain failures [9] associated with sudden price increases in essential materials such as wheat and rice, thus increasing hunger and causing serious economic disruptions. Situations such as these are very complex and they typically involve the need to balance multiple criteria in order to take effective actions to increase the systems' resiliency.

Godchalk [10] defined preparedness to sudden onset disasters as the set of "actions taken in advance of an emergency to develop operational capabilities and to facilitate response in the event that an emergency occurs" (p. 136). A system's operational risk does not only increase with the threat level, but also with the degree of vulnerability of a system [11]; the definition of resilience therefore should not only incorporate post event consequences, but also pre event preparedness and strategic planning. Resilience engineering calls for proactively looking for "ways to enhance the ability of organizations to explicitly monitor risks and to make appropriate tradeoffs between required safety levels and production and economic pressures" [12]. In resilience engineering, success is defined by "the ability of the system to monitor changing risk profile and take timely action to prevent the likelihood of damage", while failure is the "absence of this ability" [12].

The approach taken in this paper for quantifying multi event resilience is based upon the concept of the disaster resilience triangle [13]. Originally introduced by Bruneau et al. [13], the underlying construct of the disaster resilience triangle (illustrated in Fig. 1) was extended by Zobel in Refs. [3,14] to provide an approach for calculating a multi dimensional measure of predicted disaster resilience. This work also provided a means for visually comparing the tradeoffs between the multiple criteria from which the resilience measure was constructed [14], and an

* Corresponding author. Tel.: +540 231 1856.
E-mail address: czobel@vt.edu (C.W. Zobel).

0305-0548/$ - see front matter © 2011 Elsevier Ltd. All rights reserved.
doi:10.1016/j.cor.2011.09.024

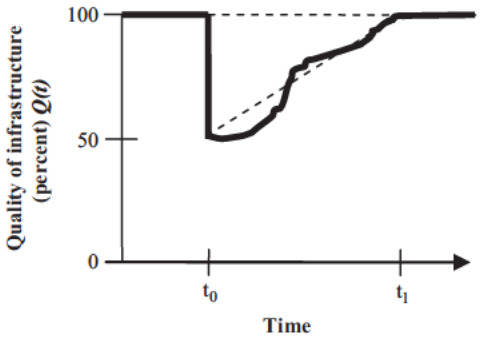

Fig. 1. Single-event resilience triangle (adapted from Ref. [13]).

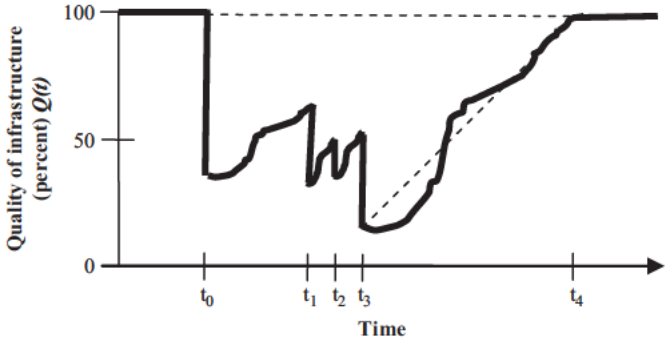

Fig. 2. Multi-event resilience graph.

approach for representing decision makers' preferences between these criteria [3].

Both Refs. [3] and [14], however, only addressed predicted resilience for a single disaster event, and the models are not sufficient to assess the resilience of a system affected by multiple related events. If a system has not had a chance to recover fully by the time the next related sub event occurs, then the characteristic shape of the disaster curve will tend to look more like Fig. 2 than like Fig. 1. In order to gain the advantages of computing an overall resilience to multiple related events, therefore, and thus to compare the predicted resilience of different systems, this paper extends the original concept of predicted disaster resilience to fit this new paradigm.

The rest of the paper is organized as follows. Section 2 presents an overview of prior work on disaster resilience, and Section 3 provides a re interpretation of predicted resilience using the partial resilience associated with each of a number of sub events. Section 4 suggests an approach for more clearly characterizing the component resilience values of these sub events, and Sections 5 and 6 provide an illustrative example of the overall technique and a discussion of the results. The paper concludes in Section 7 with a brief review of the contributions of the technique in support of effective decision making for multi criteria emergency management.

2. Background

Methods to mitigate the consequences of random system failures resulting from sudden onset disruptions have been widely investigated, and many such studies [15 17] focus on characteristics and costs specific to individual components of the systems. In contrast, the systems based literature tends to propose vulnerability mitigation strategies for systems as a whole, rather than just individual links. For example, Moghtaderi Zadeh and Der Kiureghian [18] prioritized investments in critical com ponents of a network linking civil infrastructures in order to increase overall system reliability. Similarly, Matisziw and Murray [19] developed a mathematical model based on path aggregation constraints to remedy the vulnerabilities in Ohio's interstate highway network associated with random disruptions.

Peeta et al. [20] prioritized network links by studying how each link's failure would affect the post disaster network's performance. They then justified investments in critical infra structure systems by maximizing expected network performance, post disaster, subject to budget constraints. Their model thus aimed at allocating limited funds to ensure the survivability of critical network links and their corresponding infrastructures. Liu et al. [5] also addressed the problem of allocating limited resources to improve the resilience of two complete transporta tion systems: the Sioux Falls city road network and California's Alameda County road network. The authors formulated the networks' limited resource allocation problem using a two stage stochastic programming framework.

Madni and Jackson [12] emphasized that anticipation, proac tiveness, learning (from past events), and adaptation are at the heart of estimating the resilience of a network system, and Haimes et al. [21] and Pariès [22] discussed the emergent or anticipatory characteristics of the resilience of a system of systems. Mendonça [23] also stressed that flexibility (or resour cefulness) is an important factor in resilience to disasters. The author supported the necessity of accounting for flexibility when seeking resilience through the example of police officers respond ing to the 2001 World Trade Center attack without basic tools, such as cell phones or pagers. As such, he reinforced the importance of improvisation and cognitive ability to make deci sions under pressure during an emergency. Inherent in each of these efforts is the recognized importance of quantifying the resilience of a system faced with cascading consequences.

Prior research has attempted to measure resilience in a multi tude of different settings. For example, Wang and Ip [2] conceptua lized the resilience of logistic networks in the context of aircraft maintenance and service as the "intrinsic ability [of the network] to return to a stable or normal operating state following a strong perturbation or shutdown due to serious failure or outside attack". The authors developed a measure of resilience based on the extent to which a network possesses the following three characteristics: redundancy through surplus resources, distributed supply resources, and guaranteed availability through multiple highly reliable delivery lines or paths. They then used resource optimization to select the most appropriate synthesized aircraft architecture.

Chan and Fekri [24] developed the Resiliency Connectivity metric that measures the resilience of communication networks in the face of adversarial influences. Their measure takes into account the probability of link compromise and the probability of overall network connectivity. As another example, Beroggi and Wallace [25] developed a multi expert operational risk management model for addressing unexpected threatening events or disasters.

Doumpos and Zopounidis [26] developed a multicriteria deci sion support system for bank rating in the face of financial turmoil. The authors employed the PROMETHEE method, which is used to rank various alternatives using pair wise comparisons. They took into account in their model the relative importance of the evalua tion criteria and the parameters of the evaluation process when assessing bank resilience and predicting bank failures.

Bruneau et al. [13] defined disaster resilience to be the extent to which the following factors are present within a system:

(1) Robustness the strength of the system, measured by its ability to resist the impact of a disaster event, in terms of the amount of damage suffered because of the event.
(2) Rapidity the rate at which a system is able to recover an acceptable level of functionality.

(3) Resourcefulness the level of inherent capability to dynamically respond to a disaster event, by implementing efforts to improve rapidity and/or robustness.
(4) Redundancy the extent to which components of the system may be substituted for one another when functionality has been lost or reduced.

The first two factors, robustness and rapidity, are generally considered to represent the measurable criteria by which the overall amount of resilience can be judged, and Bruneau et al. [13] defined the disaster resilience triangle (in the form of the area above the quality curve) to represent the relationship between them (see Fig. 1). The authors then associated an analytical measure for resilience with this calculated area [13]. Several authors extended this original idea by adjusting or clarifying the original formulation [27,28], and by developing performance standards for both robustness and rapidity that are used to assess the probability of achieving desired results over the course of different scenarios [29].

Zobel [14] further extended the work of Bruneau et al. [13] by explicitly considering, and representing, the tradeoffs between robustness and rapidity by introducing a new measure of *predicted resilience*. Rather than depending only on a single resilience value for each combination of these two criteria, Zobel [14] provided both a graphical and an analytical approach for differentiating between systems with identical resilience values but different levels of loss and recovery time. Zobel [3] subsequently developed an adjusted form of the predicted resilience measure by introducing an approach for representing decision makers' perceptions of the relative importance of each of the criteria within their decision making process.

Despite its ability to provide a more comprehensive representation of the multi criteria nature of disaster resilience, Zobel's predicted resilience measure is defined only for single event crisis situations (or those that can be approximated as single events). The following sections, therefore, extend this previous work by presenting an approach to calculating and representing a quantitative measure of resilience in the presence of multiple overlapping events. The discussion begins by formally reviewing the details of the predicted resilience measure, and then introducing the adjustments necessary in order to apply it under the new multi event paradigm.

3. Re-interpreting predicted resilience

As discussed above, the concept of predicted resilience [14] provides a means for analytically representing the relationship between the initial impact of, and the subsequent recovery time from, a sudden onset disaster event. If we let X represent the percentage of functionality lost, and we let T represent the time needed to recover "normal" operations, then the area of the triangle in Fig. 3 can be interpreted to represent the overall amount of time varying loss suffered by the system due to the occurrence of a particular disaster, subject to a linear rate of recovery. The predicted resilience is then determined by calculating the percentage of the total possible loss that this represents, over some suitably long time interval T^*, as follows:

$$R(X,T) = \frac{T^* \;\; XT/2}{T^*} = 1 \;\; \frac{XT}{2T^*} \quad X \in [0,1],\ T \in [0,T^*] \tag{1}$$

Fig. 3 subsequently provides a graphical illustration of the concept.

Because very different combinations of X and T could result in predicted resilience triangles with identical areas (and thus identical resilience values), Zobel [14] showed that each predicted resilience value corresponds to a rectangular hyperbola in the upper right quadrant of the plane. The set of possible predicted resilience values can therefore be represented as a series of equilateral hyperbolas, and different combinations (scenarios) of X and T can easily be differentiated and compared, as in Fig. 4.

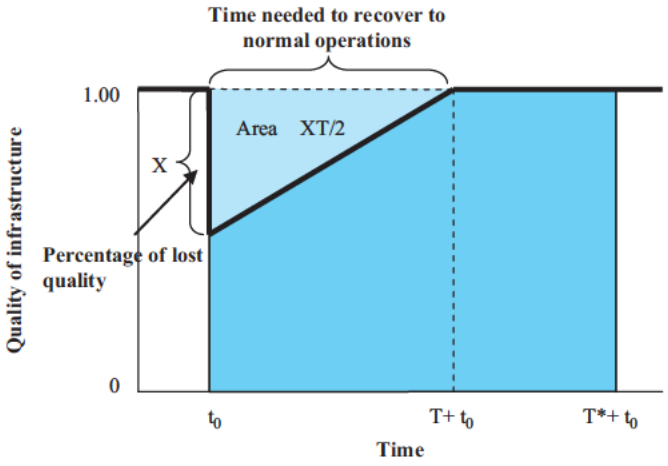

Fig. 3. Predicted resilience triangle for a single-event disaster.

X and T are point estimates of the actual initial loss and the actual recovery time (which will only be available once recovery is complete), and we assume only that they depend on the best information available in advance of the disaster event. The theoretical development of predicted resilience does not depend on any particular choice of technique for estimating these values, and in general one might expect that expert knowledge about the impacted system and its capability for recovery could be used to support these estimates. It is important to note that if the analysis is performed after the actual event has occurred, X could, of course, be assigned the actual initial loss value.

Considering the definition of predicted resilience as given in (1), suppose that instead of considering the area of the resilience triangle to be a function of X (initial loss) and T (recovery time), we consider it to be a function of $X/2$(=average loss of functionality over the period of time represented by T) and T (recovery time). This slight reinterpretation maintains the original equation but provides the basis for extending the idea of resilience to more complex situations with multiple, overlapping events. We develop the foundation for this extension as follows:

Given a compound event with n overlapping sub events, let X_i represent the total amount of loss reflected in the system immediately *after* event i occurs. Similarly, let X_i' represent the amount of loss reflected in the system immediately *before* event $(i+1)$ occurs, and let T_i represent the amount of time that it takes the system to move from the state represented by X_i to that represented by X_i'. As illustrated in Fig. 5, the average loss of functionality over the time period represented by T_i is then given by$(X_i+X_i')/2$, and the area above this portion of the curve is thus given by $A_i=(X_i+X_i')T_i/2$.

This subsequently allows us to represent the total area above the curve as the sum of these individual segments

$$A = \sum_i A_i = \sum_i (X_i + X_i')T_i/2 \tag{2}$$

Thus, following the formulation of predicted resilience, we may define the overall resilience R of the compound event as:

$$R = 1 \;\; \sum_i (X_i + X_i')T_i/2T^* \tag{3}$$

Given our definition of T_i above, the total amount of time to recovery for the entire multi event scenario is simply $T=\sum_i T_i$. By thus consolidating the time dimension of the compound event into a single value, we are subsequently able to plot the overall

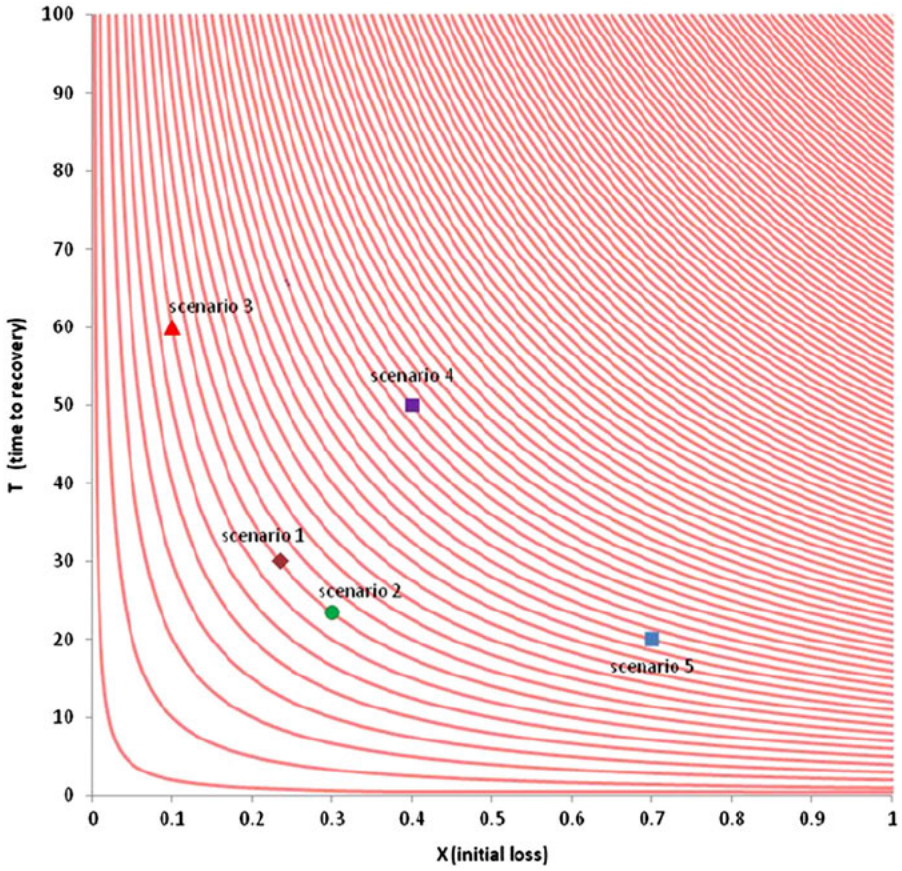

Fig. 4. Original predicted resilience curves.

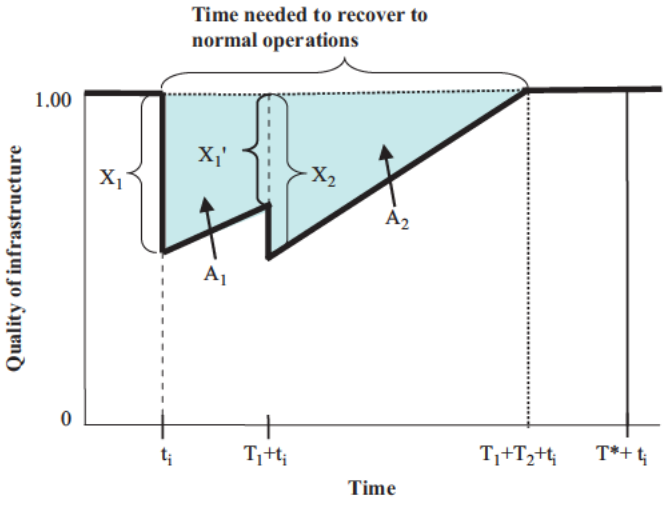

Fig. 5. Average loss of functionality with two-event disaster.

resilience of the entire event within the context of the resilience curves. We accomplish this by constructing a single event dis aster resilience triangle with a time to recovery of T and a resilience of R, and derive a unique surrogate value for the corresponding overall average loss of functionality, $X/2$, across all sub events (Eq. (4))

$$R = 1 \quad (X/2)T/T^* \Rightarrow (X/2) = (1 \quad R)T^*/T \tag{4}$$

In graphing the predicted resilience for a single event, as in Ref. [14], R is considered to be a function of X and T, and thus the horizontal axis is associated directly with X, the total initial loss associated with that event. By reinterpreting the resilience triangle in a multi event context, however, it is the *average* loss, as discussed above, which is much more descriptive of the system's behavior. This is important not only from a descriptive standpoint, but also for providing an appropriate scale upon which to compare different scenarios. In particular, although the derived value for the equivalent total amount of loss (X) in Eq. (4) may actually exceed one, the value for the corresponding average amount of loss ($X/2$) will always lie on the interval [0,1], since

$$R = 1 \quad \sum_i (X_i + X_i')T_i/2T^* = 1 \quad (X/2)T/T^*$$

$$\Rightarrow (X/2)T = \sum_i (X_i + X_i')T_i/2 \le \sum_i T_i = T \tag{5}$$

As in Refs. [14,3], we may therefore compare the total resilience for different multi event situations by using the resi lience curve approach. This supports a more complete analysis by allowing a graphical illustration of the tradeoffs between the average loss ($X/2$), and the total time to recovery (T) (see Fig. 6).

Single event resilience values may also be graphed on these new curves, and thus compared to the multi event situations, simply by plotting their average loss, ($X/2$), rather than X.

4. Characterizing partial resilience

Given that the derived concept of ($X/2$) is a surrogate measure that may correspond to a large number of different possible scenarios, it is also important to look at additional means of characterizing multi event resilience in order to be able to differentiate between such scenarios. One such approach involves introducing the concept of *partial resilience*. Given the area above

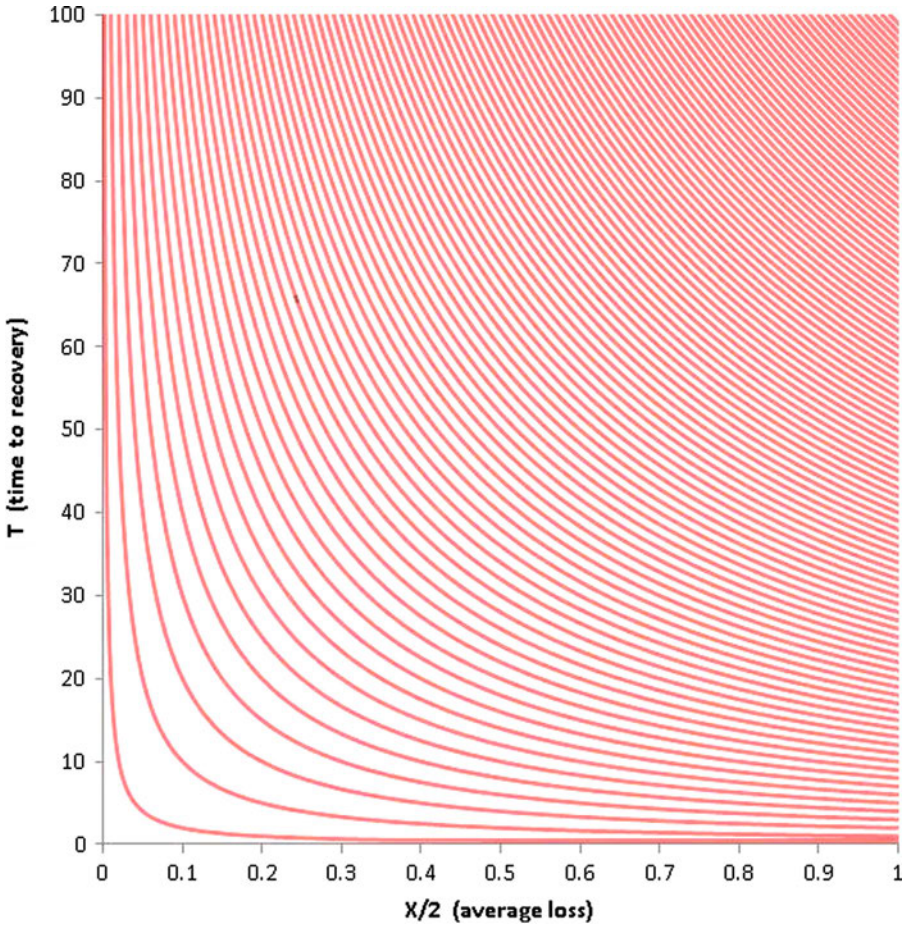

Fig. 6. Resilience curves for multi-event situations.

the curve for a particular sub event, it is relatively straightfor ward to define the resilience associated with that sub event as follows:

$$R_i = 1 \quad (X_i + X_i')T_i/2T^* \tag{6}$$

We refer to R_i as the "partial resilience" associated with event i because T_i typically only represents the time until the next sub event occurs, and not the time to full recovery as in the original predicted resilience function. It is important to note, however, that Eq. (6) can also be used to represent situations in which the system is actually able to recover from a given sub event before the next related sub event occurs. In such a situation, X_i'will be equal to zero, and T_i will represent the amount of time that it takes for the system to completely recover from that particular sub event. Eq. (3) will still hold in this case because the overall resilience is simply based on summing the areas associated with each of the sub events, regardless of the values of X_i and X_i'. We may therefore consider a multi dimensional vector representation of the total resilience in the form of its constituent partial resilience values: $(R_i,\ldots,R_n)$. Both the number of partial resilience values and their corresponding sizes would help to characterize the resilience of the situation in a more comprehensive manner than just the total resilience alone, particularly since the total multi event resilience easily can be retrieved as follows:

$$R = 1 \quad \sum_i (1 \quad R_i) \tag{7}$$

As in the case of the single event predicted resilience, however, each of these R_i values may correspond to any number of alternate scenarios with very different amounts of loss and

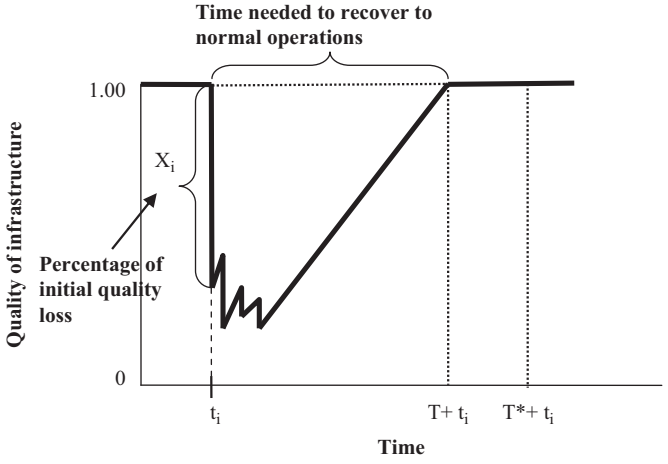

Fig. 7. Multi-event disaster with large loss but quick recovery.

time to recovery (see Fig. 7 and Fig. 8, with the same area above the curve in each case).

We may therefore consider also breaking these partial resilience values down into their component factors. Since each R_i may represent a non triangular region, it is important to keep track of each X_i and X_i', as well as each T_i. We may thus uniquely characterize each individual component of the curve by representing it as an ordered triple: (X_i,X_i',T_i), and this gives us the ability to represent the overall multi event resilience, R, by using its corresponding constitu ent set of triples: $\{(X_i,X_i',T_i)\,|\,i = 1,\ldots,n\}$. These ordered triples can be

plotted on the same resilience curves as the overall multi event resilience by recognizing that Eq. (6) simply substitutes $(X_i + X_i')$ for X and T_i for T into the equation for overall resilience that is given in Eq. (4). In each case, the given observation will be located on the resilience curve corresponding to the partial resilienceR_i. Additionally, information about X_i and X_i' may also be included by augmenting each partial resilience value with a horizontal line segment defined by the endpoints (X_i, T_i) and (X_i', T_i) (see Fig. 9). These two additional points will always be evenly spaced on either side of their corre sponding partial resilience value, and they can be used to indicate the relative amount of improvement achieved between event i and event $i+1$. It is important, however, to recognize that these two additional points do not themselves correspond to actual resilience values, since they do not explicitly depend on T_i. For this reason, we plot only the line segment, and not the actual endpoints, on the graph. It is also important to recognize that it is not necessary to augment the final sub event in this way, since typically $X_n' = 0$.

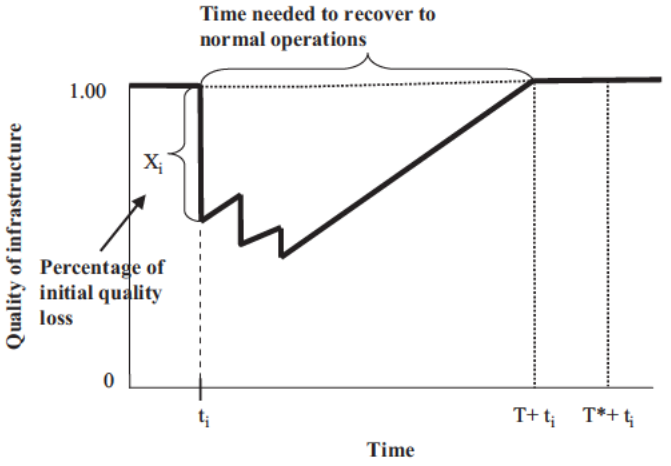

Fig. 8. Multi-event disaster with smaller loss but slower recovery.

This overall approach allows us to simultaneously graph multiple sub events for the same compound event, and thus to model the progression of the system as more events take place (A hypothetical example of a single scenario is given in Fig. 9). It also, however, allows us to compare multiple systems that are affected by a single event, such as a situation where an earthquake with aftershocks affects three different local warehouse facilities belonging to a given orga nization. Because each different system is affected by the same set of events, the partial resilience values will share the same set of T_i values, except perhaps for the recovery period following the final sub event. The comparison of the individual sub events can then focus on the relative loss due to each event, as well as on the values of X_i and X_i' and the corresponding rates of recovery $((X_i \;\; X_i')/T_i)$.

It is also possible to use this approach to compare the performance of a single system with respect to a set of different compound events. In this case, however, although the overall resilience can provide a consistent measure for comparing the total loss suffered per unit time, the individual sub events may not themselves be directly comparable if they occur on different time frames. Nevertheless, the relative sequence of partial resi lience values can still help to characterize the relative system performance in each case, and thus support a better understand ing of the system's ability to withstand and rebound from both the larger disaster event and each of the sub events with which it is associated.

As this discussion indicates, this approach to quantifying and visualizing resilience can provide a substantial amount of detail that can support differentiating between the relative resilience of differ ent multi event systems and situations. It is important to note, however, that one may not always want to make use of all this detail, and that the type of detailed information needed in a given situation will depend on the underlying scenarios and the questions to be answered. For example, if there are significant differences

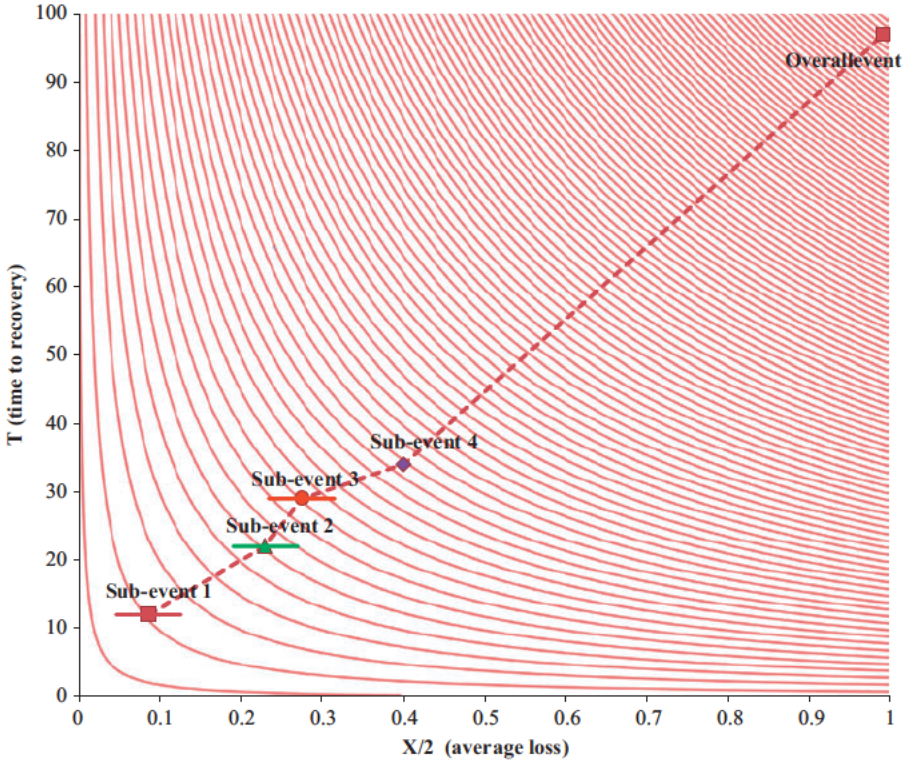

Fig. 9. Resilience for event with four sub-events.

between two systems, it may be sufficient to compare them solely on their relative multi event resilience. If further questions arise about the source of the differences, then it is at that point that a greater level of detail can then be displayed and compared. Simultaneously graphing all of the available information about each sub event, across multiple affected systems, might simply provide too much detail to be helpful to the decision making process.

5. Illustrative example

As discussed above, there are a number of different examples of systems that suffer the impacts of multiple events within the context of a larger disaster situation. In order to illustrate the application of the technique introduced above, we focus on the example of an earthquake in a heavily populated area that is subject to potential landslides and possible flooding.

Earthquakes are typically associated with aftershocks. The 2010 earthquake in Chile, for example, had 304 aftershocks of magnitude 5.0 or greater within the first two months after the initial tremor [30]. Although most structures suffer the majority of their damage in the initial tremor, structures weakened by the initial blow can eventually collapse when subjected to additional tremors [31]. There also can be significant psychological impacts on the affected population due to the uncertainty associated with the timing and impact of each succeeding aftershock [32]. The aftershocks can also lead to other types of events such as fires, landslides, and flooding. Slopes weakened by the initial shock, and lost vegetation due to fires, may be dislodged due to an aftershock, resulting in landslides that dam rivers and cause flooding [33].

Consider, for example, a subdivision of homes that is located in an earthquake prone area such as Southern California, and which is situated on a series of bluffs overlooking the ocean. Suppose that a major earthquake occurs which directly impacts this subdivision and causes varying amounts of damage to a number of the houses located there. Furthermore, suppose that eight days later, a significant aftershock occurs that causes a large landslide along one side of the subdivision, further damaging a number of houses and blocking several access routes into the neighborhood. We use the multi event resilience approach to characterize and compare five specific scenarios associated with houses affected by this hypothetical disaster situation (see Table 1).

The first representative house, described by Scenario 1, is only slightly damaged by the initial earthquake, but it is situated directly next to the area affected by the landslide and thus it suffers significant damage from the effects of the aftershock. The second house is less resistant to the earthquake and it initially suffers a great deal of damage, but it is located back from the edge of the landslide area and thus only suffers minor damage as a result of the aftershock. The third house is only somewhat protected from both the earthquake and the landslide, and thus suffers more overall damage than either of the first two houses, but it is located near the entrance to the subdivision and can be quickly and easily reached for repairs. The fourth house sustains earthquake damage similar to that of the second house, but it is located away from the landslide area and thus sustains no direct damage from the secondary event. Access to this fourth house, however, depends on a road which is completely blocked by the landslide, and thus there is a several day delay in its recovery time. Finally, the fifth house sustains partial damage from both the earthquake and the landslide, so that its total damage is equivalent to that sustained by the fourth house, but its recovery is not delayed by a road closure.

Table 1
Description of comparative resilience scenarios.

Scenario	Description
Scenario 1	Small earthquake impact and large landslide impact
Scenario 2	Large earthquake impact and small landslide impact
Scenario 3	Medium earthquake impact and medium landslide impact, more overall damage but slightly shorter recovery time because more accessible
Scenario 4	Large earthquake impact with no direct landslide impact, but access road blocked so recovery time is greater
Scenario 5	Small-to-medium earthquake impact and small-to-medium landslide impact - same total damage as that associated with large earthquake alone but less total time to recovery

Fig. 10 displays the resilience profiles for each of these five scenarios, and Table 2 provides the corresponding X_i, X_i', and T_i values, along with their measures of partial and total resilience, given $T^* = 100$ days. A constant recovery rate factor of 1 (i.e., $\Delta T/\Delta X = 1$) was specified for the time period immediately following the first event, whereas a factor of 1.2 was specified for the period following the second event because it includes recovery efforts associated with both the earthquake and the landslide.

Fig. 11 provides the multi event resilience curves for the five scenarios in Table 2. The first partial resilience values are indicated by observations that are each augmented by a horizontal line identifying the relative values of the corresponding X_1 and X_1'. These first partial resilience observations are then connected to the second partial resilience values and subsequently to the total multi event resilience values. Because it is derived by adding together each individual area (A_i), the total multi event resilience of a system is always less than that of any of its components. As discussed above, although Fig. 11 provides a great deal of information about each of the scenarios, and about the relative similarities and differences between them, it can be difficult to interpret precisely for this reason. For the sake of the following discussion and analysis, therefore, we focus on the individual components of the representation.

6. Discussion

Fig. 12 is more immediately useful than Fig. 11 as an analytical aid because it focuses on just the overall multi event resilience values. In comparing the five scenarios, we can see that scenario 5 not only has the greatest overall resilience but also it provides a good balance between the amount of damage suffered and the time to recovery. Scenario 3 has the next highest resilience value and represents a slightly quicker process of recovery, even though that facility actually suffered more damage. The graph also indicates that scenarios 1 and 4 are very similar in their resilience behavior, with the house in scenario 4 taking a slightly longer amount of time to recover. Finally, scenario 2 exhibits the least amount of resilience because it suffered the most loss and had a relatively long recovery time. Because of this long recovery time, the slight increase in average loss suffered in scenario 2 translates into a relatively large decrease in measured resilience.

Fig. 12 indicates that in order to increase the resilience of a house like that given in scenario 2, it would be more immediately effective to strengthen its resistance to loss rather than to attempt to decrease the recovery time. In order to determine which particular aspect of the loss suffered by the system is most significant, however, it is necessary to also look at the corresponding partial resilience values.

As given in Table 2 and shown in Fig. 13, the first partial resilience value for scenario 2 is tied for the lowest among the five scenarios, and the initial damage sustained (X_1) is very high. To improve the first partial resilience in the future, therefore, either X_1

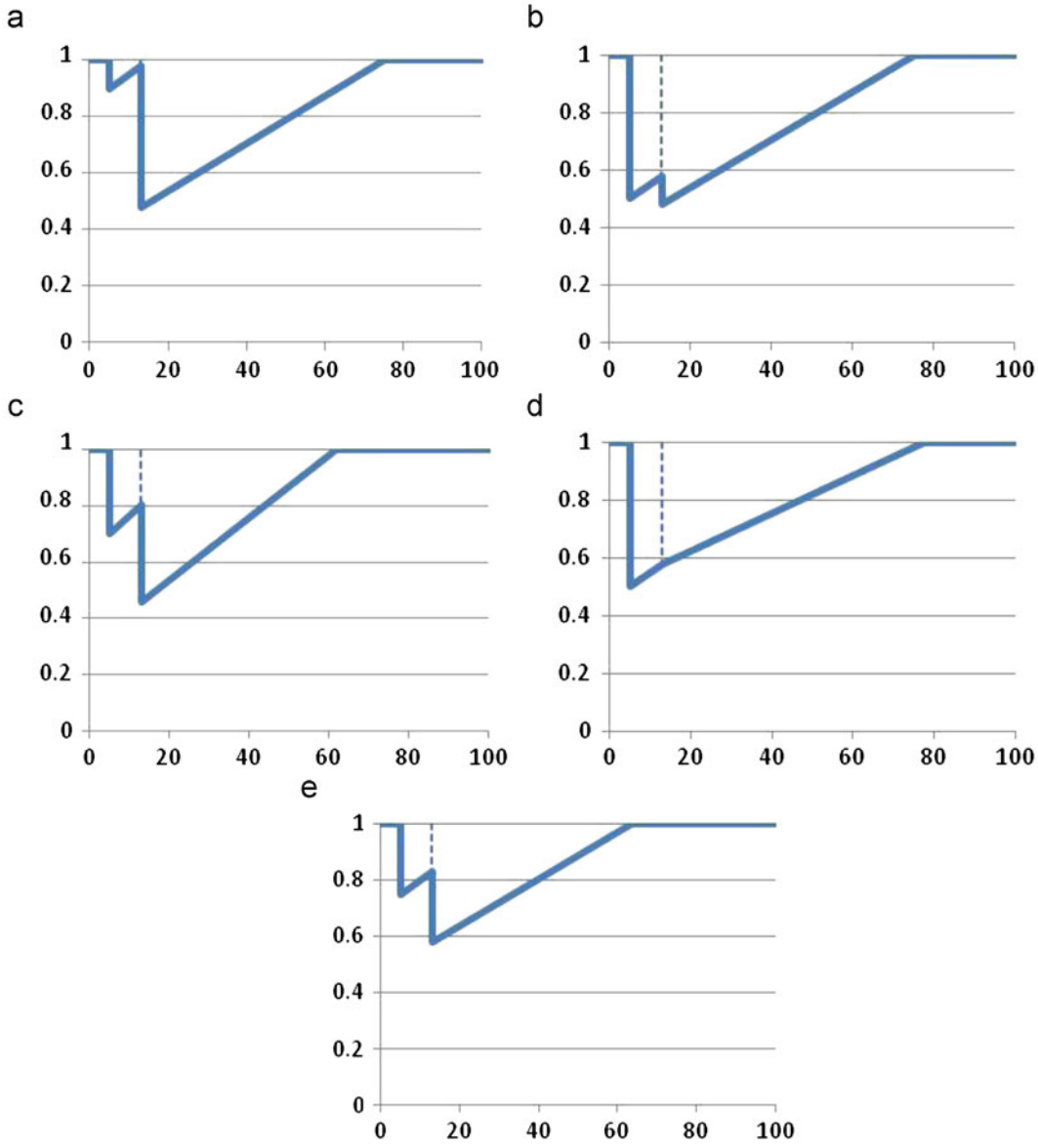

Fig. 10. Resilience profiles for the five scenarios. (a) Scenario 1: Small earthquake impact/large landslide impact. (b) Scenario 2: Large earthquake impact/small landslide impact. (c) Scenario 3: Medium impact for both/more total damage, less recovery time. (d) Scenario 4: Large earthquake impact/indirect landslide impact (longer recovery). (e) Scenario 5: Small-to-medium impact for both events/same total damage, less recovery time.

Table 2
Resilience values.

Scenario	Partial resilience 1				Partial resilience 2				Total resilience (R)
	X_1	X_1'	T_1	R_1	X_2	X_2'	T_2	R_2	
1	0.1	0.02	8	0.9952	0.52	0	62.4	0.8378	0.8330
2	0.5	0.42	8	0.9632	0.52	0	62.4	0.8378	0.8010
3	0.3	0.19	8	0.9803	0.54	0	48.9	0.8672	0.8474
4	0.5	0.42	8	0.9632	0.42	0	64.4	0.8648	0.8280
5	0.25	0.17	8	0.9832	0.42	0	50.4	0.8942	0.8774

could be decreased through mitigation or the associated recovery rate could be improved, decreasing X_1' and thus $(X_1+X_1')/2$. In the case of scenario 2, it is not very meaningful to talk about decreasing T_1 to impact the first partial resilience because this value represents the time elapsed between the earthquake and either recovery or the occurrence of the next sub event. Only scenario 1 has a value for X_1' (the lower limit of the augmented partial resilience value) indicating that recovery was almost complete ($X_1' \approx 0$) when the aftershock occurred. Scenario 1 is thus the only scenario for which T_1 might be able to be reduced, in a practical sense, by reducing X_1' to zero and thus having a more significant impact on the value of the first partial resilience.

It is important to note from Table 2 that each value for the second partial resilience (R_2) is significantly less than its correspond ing R_1, regardless of the size of event 2 relative to event 1. This relationship can easily be seen in Fig. 11 as well, and it clearly illustrates that the partial resilience is not always the same as the marginal resilience of the associated sub event. This is because the speed and trajectory of the recovery process depends on the total amount of loss exhibited by the system, and not just on the impact of the most recent sub event. Looking at the situation from an emergency manager's viewpoint, if resources are being allocated to manage recovery operations, then it is the current overall need that will typically drive that decision, and not just the need associated with the most recent disaster event. This behavior applies to any situation with more than one sub event.

Finally, it is interesting to note, in Table 2 and in Fig. 14, that scenarios 3 and 4 have very similar second partial resilience values,

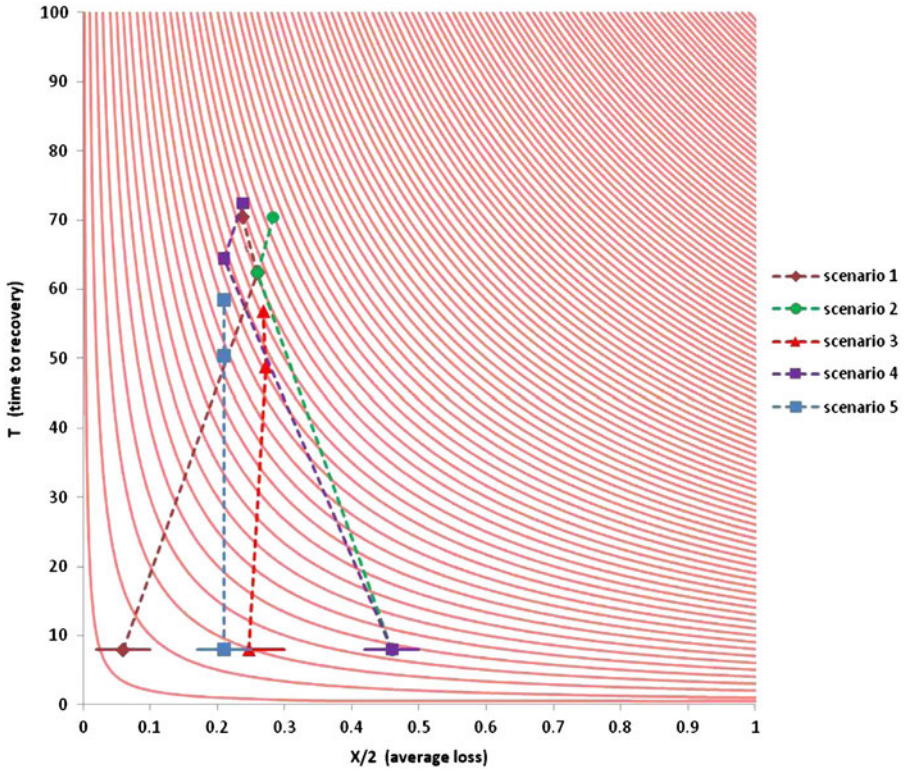

Fig. 11. Multi-event resilience for all five scenarios.

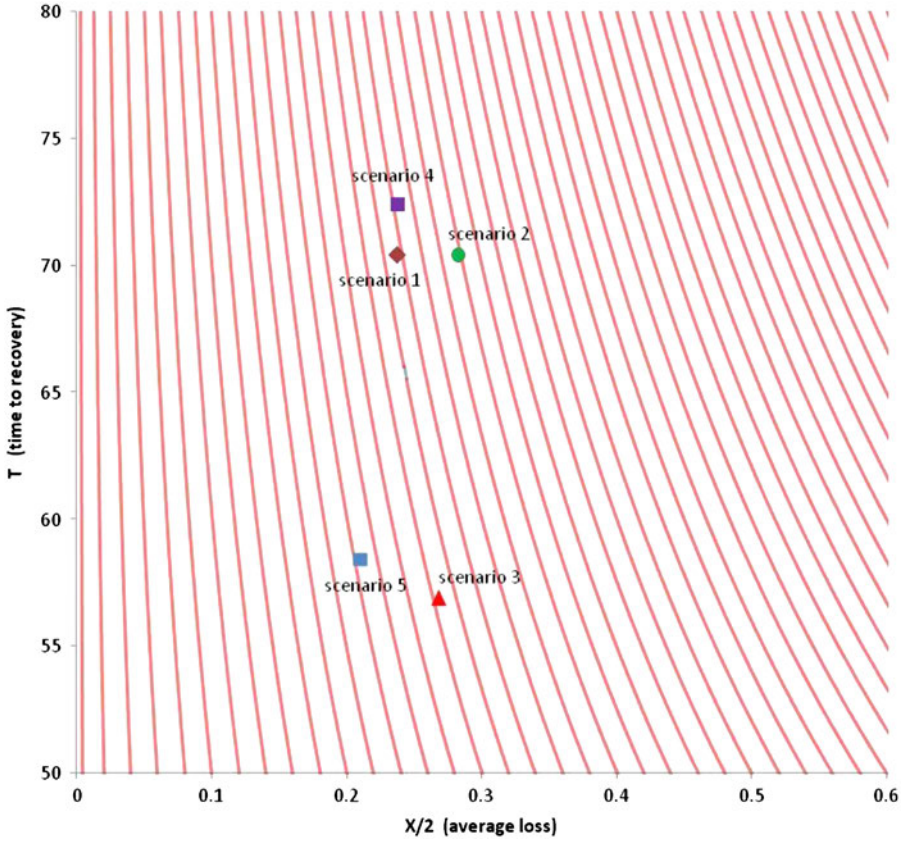

Fig. 12. Total multi-event resilience.

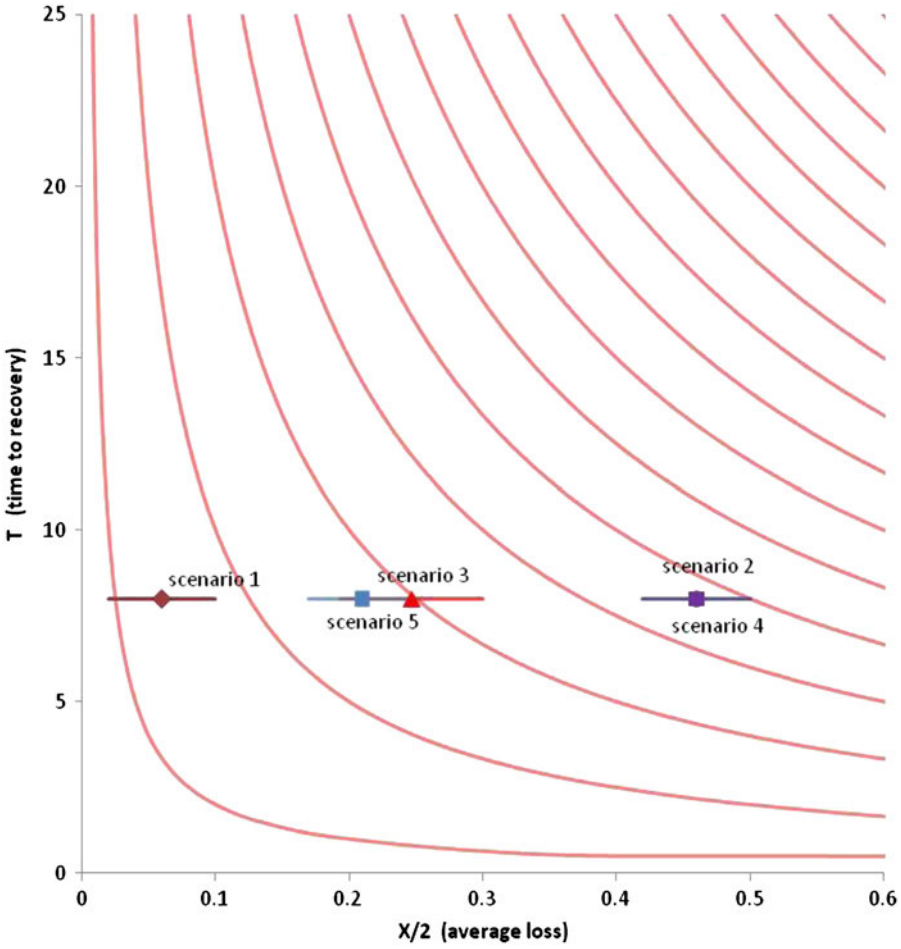

Fig. 13. Partial resilience for the time period after the first event.

even though their values for $X/2$ and T are very different from one another. This provides a nice illustration of the value of the resilience curves for examining the tradeoffs in the model between different multi criteria observations. Since the house in scenario 3 suffered a greater overall amount of damage than the house in scenario 4, and the latter only suffered direct damage from the initial earthquake, the similar second partial resilience values indicate that the loss of two days of recovery time from the road being blocked is effectively being treated as equivalent in value to the additional physical damage suffered in the third scenario. It is also important to recognize that not all decision makers would agree that these two situations are truly equivalent. In an attempt to address this potential for disagreement in the case of a single resilience triangle, Zobel [3] developed an approach for capturing a decision maker's perceptions of the true relative resilience of different situations and adjusting the predicted resilience curves to reflect *perceived* resilience. This ability to adjust the underlying model allows the resilience curves to better represent the subtleties of balancing different criteria, and thus to provide better support for actual decision making. As such, the development of an equivalent formulation for adjusted multi event disaster resilience is an impor tant future research effort.

7. Conclusions

We proposed in this paper a multi criteria approach for capturing the tradeoffs between the robustness of a system and the rapidity of its recovery, in situations involving the occurrence of multiple related disaster or emergency events. The new concept of partial resilience captures the relative time of occur rence and impact of these related events, and it provides the opportunity to both analytically and graphically represent the multi dimensional and multi criteria nature of a system under these circumstances.

Although the modeling approach being proposed is descrip tive, rather than prescriptive, in nature, its ability to numerically quantify different complex disaster scenarios can be used as the basis for comparing those scenarios on a number of different levels. Through appropriate application of MCDM techniques, a rank ordering of the scenarios could be generated in support of determining more effective mitigation or recovery plans. A similar methodology could also be used to analyze historical outcomes with respect to their relative multi event resilience. Ultimately, the strength of the approach lies in its ability to illustrate the complexity of a compound disaster event, and to help better quantify that complexity in support of more effective decision making.

It is important to recognize that the work presented in this paper is intended to provide a quantitative foundation for the further study of multi event disaster scenarios. For example, although the model itself requires point estimates for values such as the amount of loss suffered in each sub event and the time elapsed between events, these estimates could theoretically be generated by sampling from appropriate probability distributions. Rather than representing a fixed scenario determined in advance, therefore, a given resilience profile could instead represent a single quantifiable realization of a probabilistic situation. This would then

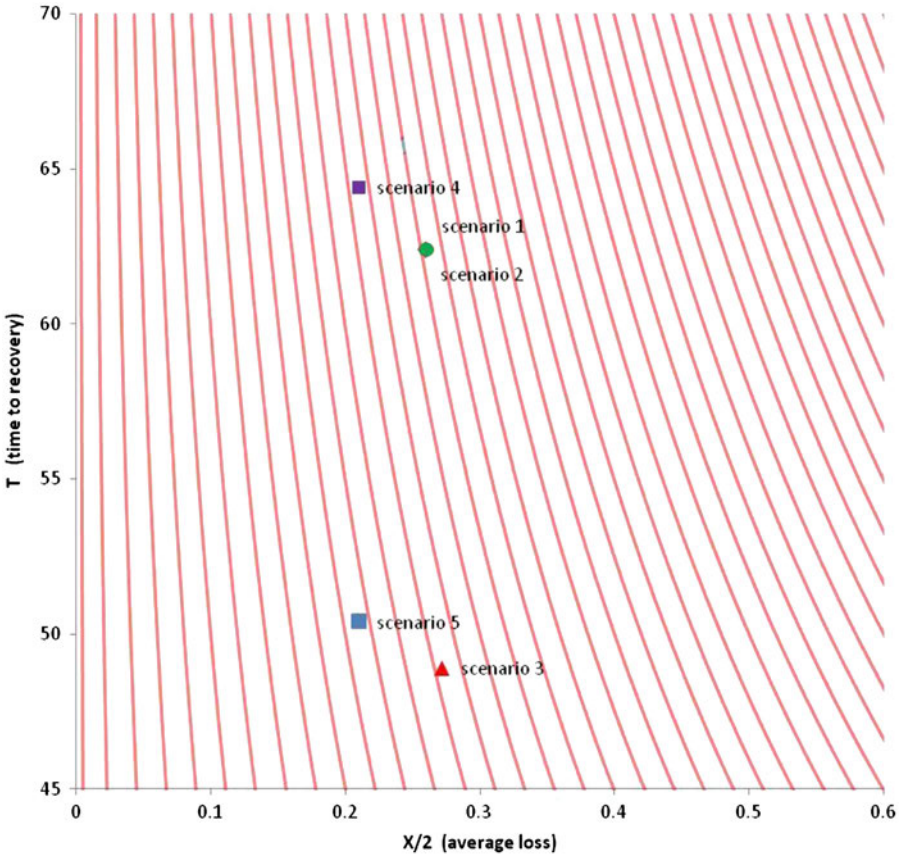

Fig. 14. Partial resilience for the time period after the second event.

allow simulation to be used to generate a statistical description of the behavior of the system, in the context of different disaster events and response capabilities. The development of appropriate techniques for incorporating such probabilistic behavior into the model is an important area of future research.

By extending the concept of predicted resilience to multi event emergencies, we enable its application to a much wider, and more realistic, variety of situations. Although models that incorporate more information are not always more helpful, they at least provide the opportunity to look at a problem in more detail, and thus hopefully support a better understanding of the complexities of the underlying systems that they are intended to represent. By supporting a variety of different views of the underlying data, and allowing the user to choose which aspects of the resilience they wish to compare, the hope is that the multi event resilience approach developed above can be, and will be, adapted as needed to fit each decision maker's individual information needs.

References

[1] Hamill JT, Deckro RF, Kloeber Jr. JM. Evaluating information assurance strategies. Decision Support Systems 2005;39:463–84.
[2] Wang D, Ip WH. Evaluation and analysis of logistic network resilience with application to aircraft servicing. IEEE Systems Journal 2009;3(2):166–73.
[3] Zobel CW. Representing perceived tradeoffs in defining disaster resilience. Decision Support Systems 2011;50(2):394–403.
[4] Snediker DE, Murray AT, Matisziw TC. Decision support for network disruption mitigation. Decision Support Systems 2008;44:954–69.
[5] Liu C, Fan Y, Ordóñez F. A two-stage stochastic programming model for transportation network protection. Computers & Operations Research 2009;36:1582–90.
[6] Scaparra MP, Church RL. A bilevel mixed-integer program for critical infrastructure protection planning. Computers & Operations Research 2008;35:1905–23.
[7] Albores P, Shaw D. Government preparedness: using simulation to prepare for a terrorist attack. Computers & Operations Research 2008;35:1924–43.
[8] Salmeron J, Wood K, Baldick R. Analysis of electric grid security under terrorist threat. IEEE Transactions on Power Systems 2004;19(2):905–12.
[9] Lau HC, Agussurja L, Thangarajoo R. Real-time supply chain control via multiagent adjustable autonomy. Computers & Operations Research 2008;35:3452–64.
[10] Godchalk DR. Disaster mitigation and hazard management. In: Drabek T, Hoetmer G, editors. Emergency management: principles and practice for local government. Washington, DC: International City Management Association; 1991.
[11] Bessani AN, Sousa P, Correia M, Neves NF, Verissimo P. The crucial way of critical infrastructure protection. IEEE Security & Privacy 2008;6(6):44–51.
[12] Madni AM, Jackson S. Towards a conceptual framework for resilience engineering. IEEE Systems Journal 2009;3(2):181–91.
[13] Bruneau M, Chang SE, Eguchi RT, Lee GG, O'Rourke TD, Reinhorn AM, et al. A framework to quantitatively assess and enhance the seismic resilience of communities. Earthquake Spectra 2003;19(4):733–52.
[14] Zobel CW. Comparative visualization of predicted disaster resilience. In: Proceedings of the seventh international ISCRAM conference. Seattle, WA; 2010.
[15] Albert R, Albert I, Nakarado GL. Structural vulnerability of the North American power grid. Physical Review E 2004;69(2):025103.1–4.
[16] Bana e Costa CA, Oliveira CS, Vieira V. Prioritization of bridges and tunnels in earthquake risk mitigation using multicriteria decision analysis: application to Lisbon. Omega 2008;36(3):442–50.
[17] Holme P, Kim BJ, Yoon CN, Han SK. Attack vulnerability of complex networks. Physical Review E 2002;65(5):056109-1–14.
[18] Moghtaderi-Zadeh M, Der Kiureghian A. Reliability upgrading of lifeline networks for post-earthquake serviceability. Earthquake Engineering and Structural Dynamics 1983;11(4):557–66.
[19] Matisziw TC, Murray AT. Modeling s-t path availability to support disaster vulnerability assessment of network infrastructure. Computers & Operations Research 2009;36:16–26.
[20] Peeta S, Salman FS, Gunnec D, Viswanath K. Pre-disaster investment decisions for strengthening a highway network. Computers & Operations Research 2010;37:1708–19.
[21] Haimes YY, Crowther K, Horowitz BM. Homeland security preparedness: balancing protection with resilience in emergent systems. Systems Engineering 2008;11:287–308.
[22] Pariès J. Complexity, emergence, resilience. In: Hollnagel E, Woods DD, Leveson N, editors. Resilience engineering: concepts and precepts. Aldershot, UK: Ashgate Press; 2006. p. 43–53.

[23] Mendonça D. Decision support for improvisation in response to extreme events: learning from the response to the 2001 World Trade Center attack. Decision Support Systems 2007;43:952–67.
[24] Chan K, Fekri FA. Resiliency-Connectivity metric in wireless sensor networks with key predistibution schemes and node compromise attacks. Physical Communication 2008;1:134–45.
[25] Beroggi GEG, Wallace WA. Multi-expert operational risk management. IEEE Transactions on Systems, Man, and Cybernetics—Part C: Applications and Reviews 2000;30(1):32–44.
[26] Doumpos M, Zopounidis C. A multicrieria decision support system for bank rating. Decision Support Systems 2010;50:55–63.
[27] Bruneau M, Reinhorn A. Exploring the concept of seismic resilience for acute care facilities. Earthquake Spectra 2007;23(1):41–62.
[28] Cimellaro G, Reinhorn A, Bruneau M. Seismic resilience of a hospital system. Structure and Infrastructure Engineering 2010;6(1):127–44.
[29] Chang SE, Shinozuka M. Measuring improvements in the disaster resilience of communities. Earthquake Spectra 2004;20(3):739–55.
[30] U.S. Geological Survey. Magnitude 8.8 – OFFSHORE MAULE, CHILE, (〈http://earthquake.usgs.gov/earthquakes/eqinthenews/2010/us2010tfan/#summary〉), last accessed on December 22, 2010.
[31] SwissRe. High risk of further damaging earthquakes in Chile (〈http://www.swissre.com/ clients/high_risk_chile.html〉), last accessed on December 20, 2010.
[32] Griffith R. Big quake aftershocks plague New Zealand city. The Independent 2010;8 (〈http://www.independent.co.uk/news/world/australasia/big-quake-aftershocks-plague-new-zealand-city-2073427.html〉), last accessed on December 22, 2010.
[33] U.S. Geological Survey. USGS Open-File report 2007-1255, (〈http://pubs.usgs.gov/of/ 2007/1255/section4.html〉), last accessed on December 20, 2010.